J Mater Sci (2010) 45:1979–1985
DOI 10.1007/s10853-009-3890-0

HTC2009

Interfacial properties of immiscible Co–Cu alloys

I. Egry · L. Ratke · M. Kolbe · D. Chatain · S. Curiotto · L. Battezzati · E. Johnson · N. Pryds

Received: 18 May 2009 / Accepted: 12 September 2009 / Published online: 1 October 2009

Abstract Using electromagnetic levitation under microgravity conditions, the interfacial properties of an $Cu_{75}Co_{25}$ alloy have been investigated in the liquid phase. This alloy exhibits a metastable liquid miscibility gap and can be prepared and levitated in a configuration consisting of a liquid cobalt-rich core surrounded by a liquid copper-rich shell. Exciting drop oscillations and analysing the frequency spectrum, both surface and (liquid–liquid) interfacial tension can be derived from the observed oscillation frequencies. This paper briefly reviews the theoretical background and reports on a recent experiment carried out on board the TEXUS 44 sounding rocket.

I. Egry (✉) · L. Ratke · M. Kolbe
Institut für Materialphysik im Weltraum, German Aerospace Center, DLR, 51170 Köln, Germany
e-mail: Ivan.Egry@dlr.de

D. Chatain · S. Curiotto
Centre Interdisciplinaire de Nanosciences de Marseille—CINaM, 13288 Marseille, France

L. Battezzati
Dipartimento di Chimica Inorganica, Chimica Fisica e Chimica dei Materiali, Universita di Torino, 10125 Torino, Italy

E. Johnson
Nano Science Center, Niels Bohr Institute, University of Copenhagen, 2100 Copenhagen, Denmark

N. Pryds
Fuel Cells and Solid State Chemistry Division, Risø National Laboratory for Sustainable Energy, Technical University of Denmark, 4000 Roskilde, Denmark

Introduction

Alloys with a metastable miscibility gap are fascinating systems due to the interplay between phase separation and solidification. In contrast to systems with a stable miscibility gap, the demixed microstructure can be frozen in by rapid solidification from the undercooled melt. Electromagnetic levitation offers the possibility to study compound drops consisting of a liquid core, encapsulated by a second liquid phase. The oscillation spectrum of such a compound drop contains information about both the surface and the interfacial tensions. The binary monotectic alloy CuCo is an ideal model system for such investigations. Its phase diagram is shown in Fig. 1.

In order to study this system, including potential industrial applications, the European Space Agency ESA funded a European project, COOLCOP [1]. In the past years, this team devoted a lot of effort to understand the behavior of such systems, starting from phase diagram calculations [2], drop dynamics [3], modeling of interfacial properties [4], and extending to solidification theories and experiments [5]. The investigations laid the ground for microgravity experiments. First results for a $Co_{25}Cu_{75}$ alloy onboard a sounding rocket are reported here.

As the temperature of a homogeneous melt of the alloy is lowered below the binodal temperature, demixing sets in and small droplets of one liquid, L1, in the matrix of the other liquid, L2, are formed. These two immiscible liquids do not consist of the pure components, but have concentrations according to the phase boundary of the miscibility gap; therefore, L1 is rich in component 1, while L2 is rich in component 2. Initially, depending on the nucleation kinetics, a large amount of liquid droplets is created. This initial phase is energetically very unfavorable, due to the high interface area created between the different drops. In the next stage,

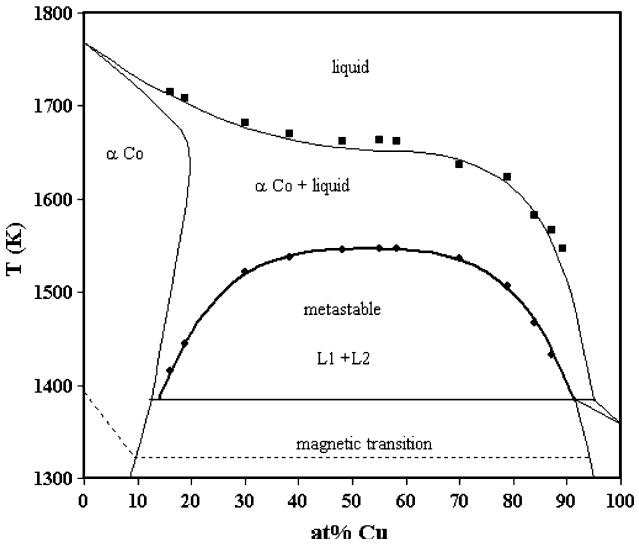

Fig. 1 Phase diagram of Cu–Co showing the metastable miscibility gap. Symbols indicate experimentally determined liquidus and binodal temperatures

Ostwald ripening sets in [6]. This diffusive mechanism leads to the growth of large drops at the expense of the small ones, thereby coarsening the structure of the dispersion and finally leading to two separated liquid phases. For a levitated drop, without contact to a substrate, the liquid with the lower surface tension—in the present case the copper-rich liquid—encapsulates the liquid (cobalt-rich) core.

Terrestrial levitation experiments suffer from the detrimental side effects of the levitation field, in particular by electromagnetic stirring effects which destroy the separated two-phase configuration. Therefore, it was decided to perform such an experiment under microgravity conditions on board a TEXUS sounding rocket. As will be discussed below, the drawback of this carrier is the short available experiment time of about 160 s. Due to a specific preparation of the sample, it was nevertheless possible to conduct three melting cycles during this short time.

Drop dynamics

Generally speaking, the interfacial tension between two liquids is difficult to measure, and only few data exist in Ga-based [7, 8] and Al-based [9–11] binaries, where the miscibility gap is stable. The oscillating drop technique [12] is a noncontact measurement technique for surface tension measurements of levitated liquid drops. It allows to investigate metastable systems and high temperature ranges thanks to the absence of container. In its original form, it assumes a homogeneous nonviscous drop, free of external forces. In this ideal case, the frequency of surface oscillations is simply related to the surface tension σ_0 by Rayleigh's formula [13]:

$$\omega_0^2 = \frac{8\sigma_0}{\rho_0 R_0^3} \tag{1}$$

where ρ_0 is the density of the drop and R_0 its radius. By substituting $\rho_0 R_0^3 = 3\ M/4\pi$, the apparent density dependence of the frequency disappears which makes this equation particularly easy to use.

In the case of a viscous drop, the damping of the oscillations is related to the viscosity [14]. As long as the viscosity is small enough, it has no influence on the oscillation frequency [15].

The oscillating drop technique can be extended to the measurement of the interfacial tension between two immiscible liquids [3]. Based on the theory of Saffren et al. [16], the theory was worked out for force-free, concentric spherical drops.

The geometry considered is summarized in Fig. 2. Due to the presence of the interface between liquid L1 and L2, this system possesses two fundamental frequencies, driven by the surface tension σ_0 and the interfacial tension σ_{12}.

Adopting the nomenclature of [16], the normal mode frequencies ω of a concentric, force-free, nonviscous compound drop read:

$$\omega_{\pm}^2 = K_{\pm}\frac{W}{J} \tag{2}$$

K and J are dimensionless, while W is a frequency squared. W/J is given by:

$$\frac{W}{J} = \frac{\omega_0^2\tau^8}{\sigma}\frac{1}{(1+\Delta\rho_i)\tau^{10} + 2/3\Delta\rho_i} \tag{3}$$

Here, a number of symbols have been introduced which are defined as follows:ω_0 is the unperturbed Rayleigh

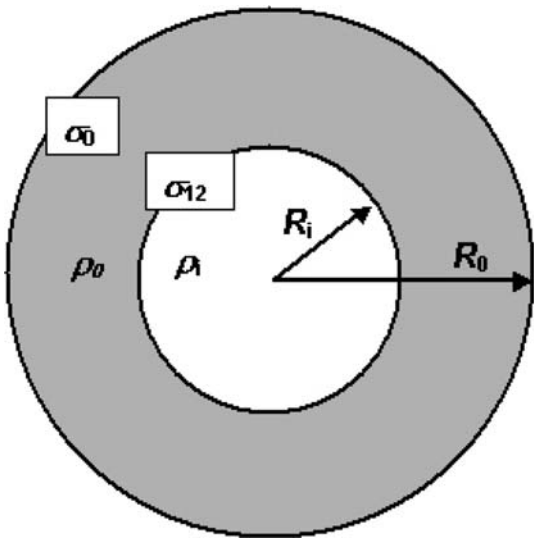

Fig. 2 Cross section of a spherical, concentric compound drop consisting of two immiscible liquids with densities ρ_i and ρ_0, radii R_0 and R_i, surface tension of the outer liquid σ_0, and interfacial tension σ_{12}

frequency (Eq. 1) of a simple drop with density ρ_0, Radius R_0, and surface tension σ_0 (see also Fig. 2 for the definition of the symbols).

$$\tau = \sqrt{\frac{R_0}{R_i}} \tag{4}$$

is the square root of the ratio between outer and inner radius,

$$\sigma = \sqrt{\frac{\sigma_0}{\sigma_{12}}} \tag{5}$$

is the square root of the ratio of the surface tension and the interface tension, and

$$\Delta\rho_i = \frac{3}{5}\frac{\rho_i - \rho_0}{\rho_0} \tag{6}$$

is the weighted relative density difference between liquids L1 and liquid L2. It remains to write down the expression for K. It is given by:

$$K_\pm = \frac{1}{2}\left(\frac{\sigma m_i}{\tau^3} + \frac{m_0\tau^3}{\sigma}\right) \pm \sqrt{\frac{1}{4}\left(\frac{\sigma m_i}{\tau^3} - \frac{m_0\tau^3}{\sigma}\right)^2 + 1} \tag{7}$$

where two additional symbols have been introduced, namely:

$$m_0 = \frac{3}{5}\tau^5 + \frac{2}{5}\tau^{-5} \tag{8}$$

and

$$m_i = (1 + \Delta\rho_i)\tau^5 - \Delta\rho_i\tau^{-5} \tag{9}$$

For large σ and small $\Delta\rho_i$, approximate equations can be derived for the two frequencies ω_+ and ω_-:

$$\omega_+^2 = \omega_0^2\left(1 + \frac{1}{\sigma^2\tau^4}\right) \tag{10}$$

$$\omega_-^2 = \omega_0^2\frac{\tau^6}{\sigma^2}\left(1 - \frac{5}{3}\tau^{-10}\right) \tag{11}$$

From an experimental point of view, it is interesting to discuss the frequencies as a function of the initial, homogeneous composition of the drop. To this end, we introduce the relative mass fraction of component 2, i.e., the component with the lower surface tension which will eventually constitute the outer liquid shell. It is given by:

$$m_{rel} = \frac{m_{shell}}{m} = \left(1 + \frac{R_i^3 \quad \rho_i}{R_0^3 - R_i^3\rho_0}\right)^{-1} \tag{12}$$

In Fig. 3, the frequency spectrum is shown as a function of m_{rel} for parameters corresponding to the Cu–Co system.

Although the oscillations of the inner radius, R_i, cannot be observed optically for nontransparent liquid metals, both eigenfrequencies can be determined from the oscillations

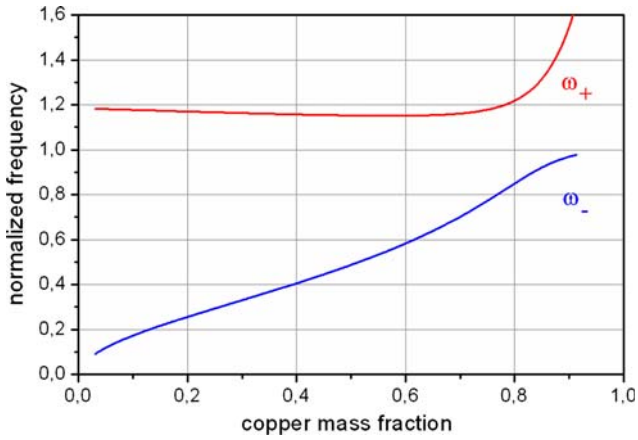

Fig. 3 The normalized normal mode frequencies $\omega_\pm/\omega_0$ as a function of the relative mass fraction m_{rel}. For the figure, following parameters were chosen: $\sigma_0 = 1.3$ N/m, $\sigma_{12} = 0.5$ N/m, $\rho_0 = 7.75$ g/cm^3, and $\rho_i = 7.86$ g/cm^3

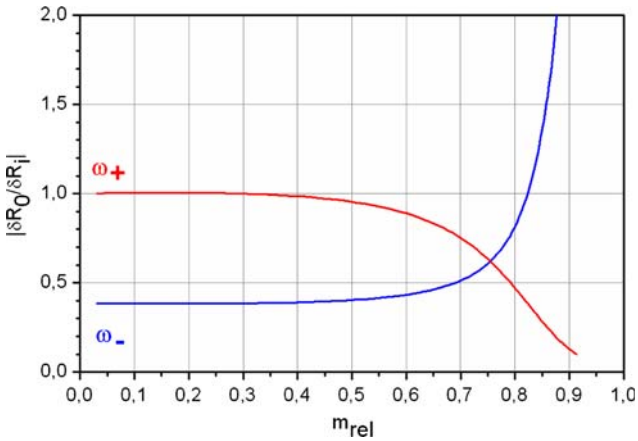

Fig. 4 Relative amplitudes of the oscillations of inner and outer surface as a function of mass fraction for both modes

of the outer radius, R_0, alone. This is due to the coupling of the two oscillators via the common velocity field in the melt. The relative amplitudes of the oscillations of the outer and inner surface are shown in Fig. 4 for both oscillatory modes. The larger the value of $|\delta R_0/\delta R_i|$, the better the detectability. Consequently, the optimal choice to detect both modes, lies between $0.7 < m_{rel} < 0.8$.

Results

The experiments were carried out using the TEXUS-EML module during the TEXUS 44 campaign. Two experiments, one on demixing of CuCo, described here, and one on calorimetry and undercooling of an Al–Ni alloy were

accommodated. The allotted time span of microgravity for the present experiment was 160 s.

As this time is much too short for undercooling and complete phase separation, it was decided to perform the experiment on a sample which was prepared ex situ as a two-phase compound drop using a DTA furnace and a melt flux technique which allows deep undercooling and subsequent phase separation of the Cu–Co sample [17]. Of course, such a system is not in equilibrium when it is remelted, but it takes some time to destroy the interface between the two liquids L1 and L2, and this time is sufficient to excite and observe oscillations of the (unstable) interface.

The experiment consisted of three heating cycles:

- one cycle with a completely phase-separated sample
- one cycle with a homogenized sample
- one cycle for maximum undercooling

The experiment was conducted with one sample of the composition $Cu_{75}Co_{25}$ with a pre-separated microstructure. Careful heating should melt the Cu shell first and then, at higher temperature, the Co core. The aim of the experiment was to observe the oscillations of this separated microstructure in the liquid and to experimentally determine the interface energy of Cu–Co. In a second heating cycle, the microstructure was homogenized and two pulses were applied to observe oscillations of a homogeneous sample for comparison. A third heating cycle was used to investigate growth of a droplet dispersion starting after undercooling at the binodal.

The most important parameter in the preparation of the experiment was the choice of the maximum temperature in the first heating cycle. It had to be chosen such that both, the outer copper shell, and the inner cobalt core are fully molten, but not intermixed. Microstructure analysis of the samples from previous parabolic flights has shown that a maximum temperature of 2,073 K of the heating cycle was too high, as the pre-separated microstructure has been destroyed. On the other hand, a minimum temperature of about 1,773 K is required to melt the cobalt-rich core. Consequently, a maximum temperature of 1,873 K has been chosen for the TEXUS experiment.

The experiment was successful and three heating cycles could be conducted. The second cycle led probably to homogenization of the liquid sample ($T_{max} \approx 2{,}123$ K). Two heating pulses for excitation of the homogeneous droplet oscillations have been applied in the high temperature region. The third cycle led to an undercooling of the melt and a recalescence due to release of latent heat, which is indicated by an arrow in the temperature–time profile in Fig. 5. The sample was saved and the experiment with Cu–Co was finished.

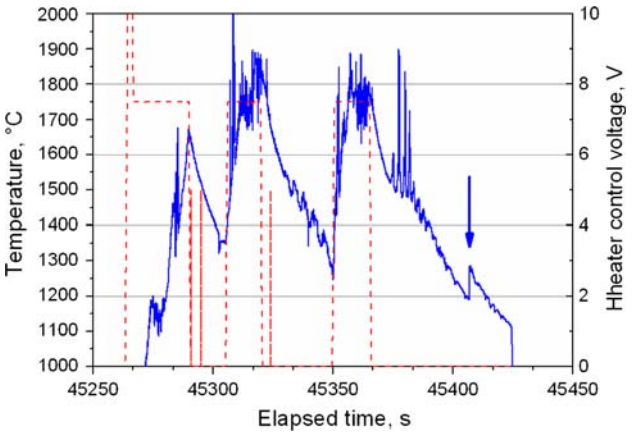

Fig. 5 Temperature-time profile of the Cu–Co TEXUS 44 experiment. *Dotted lines* show the heater activity, not all pulses are shown due to the time resolution of the display. The *arrow* indicates final solidification

Discussion

Temperature calibration

The emissivity of the sample changes depending on whether or not it is phase separated. The pyrometer data were calibrated for $\varepsilon = 0.1$, corresponding to a demixed sample. It is assumed that the second heating homogenizes the sample, leading to a depletion in copper at the surface and, consequently, an increase of the emissivity to $\varepsilon = 0.13$. These emissivity values were determined experimentally in previous parabolic flights by identifying the liquidus temperatures of demixed and homogeneous liquid samples. They also agree reasonably well with estimates based on a linear interpolation between the emissivities of copper and cobalt. Therefore, the pyrometer signal had to be corrected for the second and subsequent cycles according to:

$$\frac{1}{T_1} - \frac{1}{T_2} = \frac{\lambda_0}{c_2} \ln \frac{\varepsilon_1}{\varepsilon_2} \tag{13}$$

where λ_0 is the operating wavelength of the pyrometer, and $c_2 = 1.44 \times 10^4$ μm K.

The pyrometer operates in a band of 1.45–1.8 μm. Assuming an effective wavelength of $\lambda_0 = 1.5$ μm results in a correction of -2.733×10^{-5} K^{-1}. We estimate that the uncertainty in temperature measurement is about 20 K, or 1%.

Taking this correction into account, the pyrometer signal was recalibrated and is shown in Fig. 5. Also shown (dashed line) is the heater control voltage, controlling the heating power in the coil system of the EML module. The sample is molten within 30 s, between 45,260 and 45,290 s. During cooling, short heater pulses are applied to excite oscillations of the liquid drop. Due to the time

resolution of the data acquisition, not all such pulses are shown in Fig. 5.

The temperature signal is rather noisy, especially during heating. This is due to sample movement and sample rotation. As explained above, the sample was prepared in a melt flux, and part of this flux was still attached to the sample surface. This flux has a much higher emissivity than the metallic sample. Whenever such a clod of glass entered the measuring spot of the pyrometer, its signal went up, resulting in spikes. In fact, the temporal distance of these spikes is a quantitative measure of the sample's rotation frequency. Compared to the total surface area of the droplet and the wavelength of the surface oscillations, the area covered by the flux is very small. Therefore, the effect on the surface oscillation frequencies is negligible. Obviously, there is no effect on the oscillations of the liquid–liquid interface.

The solidus temperature is, according to the phase diagram, $T_s = 1{,}353$ K and is visible in the signal around 45,280 s. After the final sequence, the sample undercooled and solidified at 45,410 s, displaying a recalescence peak. Undercooling relative to the corresponding liquidus temperature was about $\Delta T = 200$ K.

Oscillation spectra

For the analysis of the spectra, a number of sample parameters need to be known. First of all, the mass was determined before and after the flight. The sample mass was $M_0 = 1.31$ g. The masses of copper and cobalt were $M_{Cu} = 1.00566$ g, $M_{Co} = 0.3064$ g, resulting in 76.65 wt% copper.

For the evaluation of the oscillation frequencies, the radius in the liquid phase is required. This cannot be measured directly, and we estimate it from the sample mass according to

$$R_{\text{eff}} = \sqrt[3]{\frac{3M}{4\pi\rho}} \tag{14}$$

The densities of liquid copper and cobalt were measured by Saito and coworkers [18, 19]. At the melting point, the quoted values are: $\rho_{Cu}(T_m) = 7.86$ g/cm^3, $\rho_{Co}(T_m) = 7.75$ g/cm^3. The temperature dependent densities are as follows:

$$\rho_{Co}(T) = 9.71 - 1.11 \times 10^{-3}\ \text{T g/cm}^3$$

$$\rho_{Cu}(T) = 8.75 - 0.675 \times 10^{-3}\ \text{T g/cm}^3$$

At $T = 2{,}000$ K, we obtain $\rho_{Co}(2{,}000\ \text{K}) = 7.49$ g/cm^3 and $\rho_{Cu}(2{,}000\ \text{K}) = 7.44$ g/cm^3. As these two densities are very close, we have decided to neglect the density difference and to assume $\rho_{Co} = \rho_{Cu} = 0.765\rho_{Cu}(2{,}000\ \text{K}) + 0.235\rho_{Co}(2{,}000\ \text{K}) = 7.45$ g/cm^3 throughout the analysis. Inserting this value into above equation, we obtain

$$R_{\text{eff}} = R_0 = 3.475\ \text{mm}$$

We still need to determine m_{rel} and R_i. For these two quantities, we need to know the compositions of the two separated liquids L1 and L2. This of course depends on the solidification path and is not known a priori. From EDX analysis of samples prepared identically to the flight sample, we estimate that the L2 liquid consists of approximately 90 wt% copper and 10 wt% cobalt, while L1 is composed of 16 wt% copper and 84 wt% cobalt. We therefore estimate $m_{rel} = (1.31)^{-1}$ and obtain $R_i = R_0\sqrt[3]{1 - m_{rel}} = 2.149$ mm.

In order to get a feeling for the oscillation frequencies, we need estimates for the surface and interfacial tensions. The surface tensions of the Cu–Co system have been measured by Eichel and Egry [20]. For the composition $Cu_{70}Co_{30}$ which is very close to our sample, their result is:

$$\sigma_0(T) = 1.22 - 0.29 \times 10^{-3}(T - 1{,}638\ \text{K})\,\frac{N}{m}$$

For $T = 1{,}938$ K, this yields $\sigma_0 = 1.13$ N/m. Inserting this into the Rayleigh equation, Eq. 1, we obtain a Rayleigh frequency

$$\nu_0 = \omega_0/(2\pi) = 27.06\ \text{Hz}.$$

For the interfacial tension, we assume complete wetting, yielding $\sigma_{12} = \sigma_{L1} - \sigma_{L2}$. From [20], we have:

$$\sigma(Cu_{15}Co_{85}) = 1.4 - 0.2 \times 10^{-3}(T - 1{,}713\,K)\,\frac{\text{N}}{\text{m}}$$

$$\sigma(Cu_{90}Co_{10}) = 1.22 - 0.29 \times 10^{-3}(T - 1{,}638\,K)\,\frac{\text{N}}{\text{m}}$$

At 1,938 K, we obtain:

$$\sigma_{12} = 0.225\,\frac{\text{N}}{\text{m}}$$

Inserting these values into Eq. 2, we obtain

$$\nu_+ = 28.75\ \text{Hz}, \ldots \nu_- = 17.26\ \text{Hz}$$

for a separated two-phase drop.

Surface tension

As pointed out before, sample oscillations were excited by short current pulses through the heating coil, which led to a compression and subsequent damped oscillations of the sample. The sample shape was recorded by a video camera, looking along the symmetry axis of the sample (top view) operating at 196 Hz.

The obtained images were analysed off-line by image processing with respect to a number of geometrical parameters; the most important ones are: area of the visible cross section and radii in two orthogonal directions. From the latter, two more parameters can be constructed, namely

the sum and the difference of these two radii. In case of nonspherical samples, the latter should have slightly different peaks in their oscillation spectra [21], while the Fourier spectrum of the area signal should contain all peaks. Although there were no big differences between the signals, the area signal was used for further analysis. The time signals of these oscillations are shown in Fig. 6 for the first melting cycle. In the first cycle, three oscillations are clearly visible, but the first one is somewhat disturbed. The second cycle also shows three oscillations; they are not shown here.

In order to obtain the oscillation frequencies, each oscillation was analysed separately by performing a Fourier transformation. The result is shown in Fig. 7 for all pulses analysed.

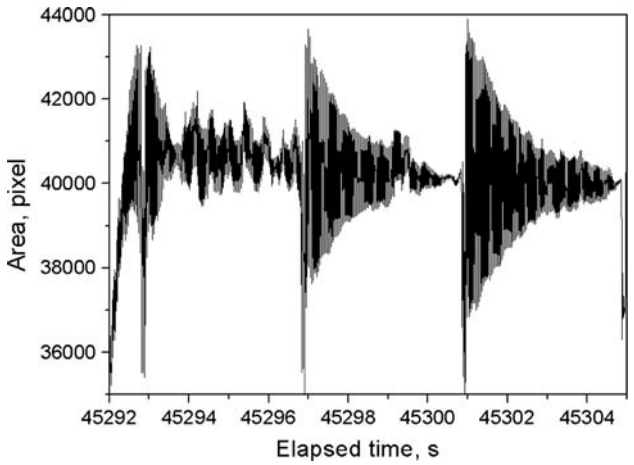

Fig. 6 Oscillations of the visible cross section during the first melting cycle

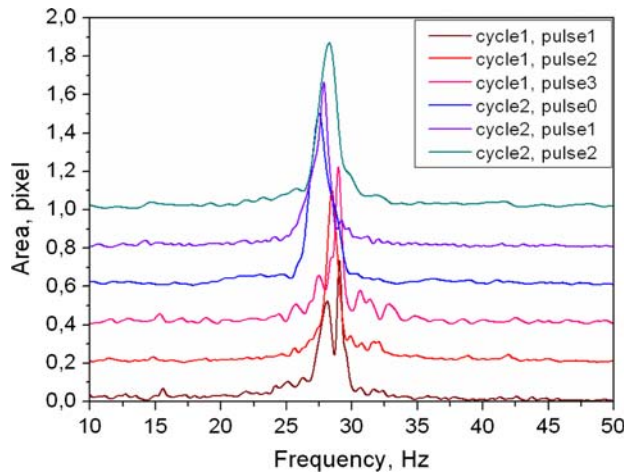

Fig. 7 Fourier transforms of the area signal for all evaluated pulses. The spectra are shifted vertically for clarity. From *bottom* to *top*: cycle1/pulse 1, cycle 1/pulse 2, cycle 1/pulse 3, cycle 2/pulse 0, cycle 2/pulse 1, and cycle 2/pulse 2

Except for the first pulse of the first cycle, all spectra display a single peak around 28 Hz. The first pulse of the first cycle displays two peaks at 28 Hz, and a small peak around 15 Hz. Positions and corresponding temperatures of the main peaks are shown in Table 1. Assuming that, after the first pulse, the sample is single phase, these frequencies correspond to the Rayleigh frequency (Eq. 1). We then obtain the surface tension as a function of temperature, as shown in Fig. 8. Linear fit to the data yields

$$\sigma(T) = 1.29 - 2.77 \times 10^{-4}\,(T - 1{,}630\,\mathrm{K})\ \mathrm{N/m} \qquad (15)$$

This is in excellent agreement with the data measured by Eichel and Egry [20]. The uncertainty is about 5% for the absolute value and about 20% for the temperature coefficient.

As is evident from Figs. 6 and 7, the oscillations during the first pulse of the first cycle are more complex than for

Table 1 Temperatures and peak positions of the pulsed oscillations

Pulse	Temperature, K	Frequency, Hz	Remarks
Cycle 1 Pulse 1	1,863	28.6	Split peak (28.1 + 29.06)/2
Cycle 1 Pulse 2	1,763	28.7	
Cycle 1 Pulse 3	1,683	28.8	
Cycle 2 Pulse 0	2,023	27.8	
Cycle 2 Pulse 1	1,933	28.0	
Cycle 2 Pulse 2	1,843	28.3	

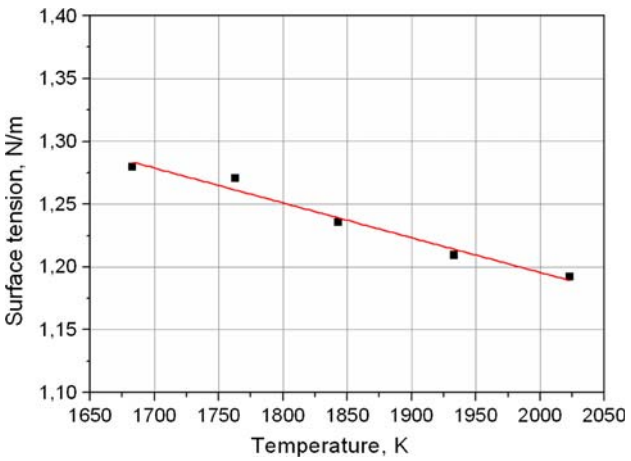

Fig. 8 Surface tension of $Cu_{75}Co_{25}$ alloy

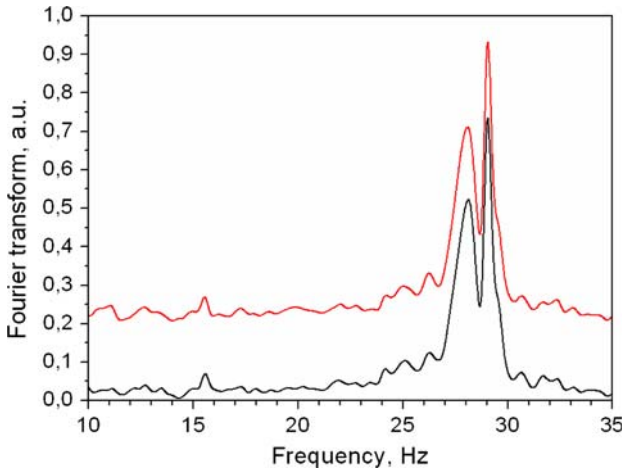

Fig. 9 Fourier spectra of the first pulse in the first cycle. FFT of cross section (*top*) and radius sum (*bottom*) is shown. Spectra are shifted vertically for clarity

the other pulses. We have therefore analysed this pulse in greater detail, as shown Fig. 9. Regardless of the parameter analysed, two peaks around 29 and 28 Hz and a small peak at 15 Hz are clearly visible. Therefore, we conclude that the liquid drop was initially phase separated, giving rise to two peaks around 15 and 29 Hz, and homogenized in the course of the oscillations yielding the Rayleigh frequency at 28 Hz.

If this is correct, we must be able to fit all three frequencies by two values for the surface tension σ_0 and the interfacial tension σ_{12}. This is shown in Table 2. Note that the uncertainty in determining the oscillation frequency is about 0.1 Hz. From the fit we obtain:

$$\sigma_0 = 1.21 \text{ N/m}, \quad \sigma_{12} = 0.17 \text{ N/m}$$

The value for the surface tension corresponds to 1,863 K and agrees well with the fit obtained from the other pulses (see Fig. 8). The value of the interfacial tension is somewhat lower than previously estimated. This may be due to a slight shift in the compositions of the two liquids L_1 and L_2, which, as mentioned before, are not known precisely. Also, we cannot exclude that partial homogenization of the phase separated drop has already taken place during the first cycle, which would lead to a decrease in interfacial tension. Therefore, the major uncertainty lies in the determination of the composition, rather than in the measurement of the interfacial tension itself.

Table 2 Measured and calculated frequencies for the first pulse of the first cycle

	Measured	Calculated
ν_0	28.1 ± 0.1	28.0
ν_+	29.1 ± 0.1	29.1
ν_-	15.5 ± 0.1	15.4

Summary

Using the EML module on board the TEXUS 44 microgravity mission, a $Co_{25}Cu_{75}$ sample was successfully processed. Following results were obtained:

- surface tension as function of temperature
- interfacial tension at 1,863 K
- size distribution of precipitated Co drops

The interfacial tension could not be measured as a function of temperature because the unstable interface was destroyed during the first pulse. The final and decisive experiment will have to be performed on board the ISS, when time is sufficient to keep the sample in the undercooled phase until complete phase separation is obtained and a metastable interface exists between the two liquid phases.

Acknowledgements The authors thank the EADS team in Bremen and Friedrichshafen, the launch team at Esrange, and, last but not least, the DLR-MUSC team for their continuous and excellent support. The authors also would like to thank ESA for providing this flight opportunity. Without their help, this experiment would not have been possible.

References

1. Egry I, Herlach D, Kolbe M, Ratke L, Reutzel S, Perrin C, Chatain D (2003) Adv Eng Mater 5:819
2. Curiotto S, Battezzati L, Johnson E, Pryds N (2007) Acta Mater 55:6642
3. Egry I (2002) Z Metallkd 93:528
4. Antion C, Chatain D (2007) Surf Sci 601(10):2232
5. Zhao JZ, Kolbe M, Gao LL, Gao JR, Ratke L (2007) Met Trans A 38:1162
6. Ratke L (1993) In: Ratke L (ed) Immiscible liquid metals and organics. DGM, Oberursel
7. Chatain D, Vahlas C, Eustathopoulos N (1984) Acta Metall 32:227
8. Chatain D, Martin-Garin L, Eustathopoulos N (1982) J Chim Phys 79:569
9. Merkwitz M, Weise J, Thriemer K, Hoyer W (1998) Z Metallkd 89:247
10. Merkwitz M, Hoyer W (1999) Z Metallkd 90:363
11. Kaban I, Hoyer W, Merkwitz M (2003) Z Metallkd 94:831
12. Egry I (1991) J Mater Sci 26:2997. doi:10.1007/BF01124834
13. Rayleigh L (1879) Proc R Soc Lond 29:71
14. Chandrasekhar S (1961) Hydrodynamic and hydromagnetic stability. Clarendon Press, Oxford
15. Suryanarayana P, Bayazitoglu Y (1991) Int J Thermophys 12:137
16. Saffren M, Ellmann D, Rhim W-K (1981) In: Le Croisette D (ed) Proceedings of the 2nd international colloquium on drops and bubbles, Monterey
17. Willnecker R, Wittmann K, Görler G (1993) J Non-Cryst Sol 156–158(1):450
18. Saito T, Amatu M, Watanabe S (1971) Trans JIM 12:17
19. Watanabe S, Saito T (1972) Trans JIM 13:186
20. Eichel R, Egry I (1999) Z Metallkd 90:371
21. Cummings D, Blackburn D (1991) J Fluid Mech 224:395